Sonochemical Synthesis of the Novel 1d Zig-zag Hg(Ii)-iodo Brigdged Metal-organic Coordination Compounds With Thiosemicarbazide Derivative Ligand

Younes Hanifehpour
Sayyed Jamaleddin Asadabadi University
Jaber Dadashi
Faculty of Science, University of Qom
Mohammad Khaleghian
Faculty of Science, University of Qom
Mahboube Rezaei
Faculty of Science, University of Qom
Babak Mirtamizdoust (babakm.tamizdoust@gmail.com)
University of Qom
Sang Woo Joo
Yeungnam University

Research Article

Keywords: Crystal structure, Coordination polymer, Hg (II) complex, Structural characterization, Ultrasonic irradiation

Posted Date: May 11th, 2021

DOI: https://doi.org/10.21203/rs.3.rs-504984/v1

Version of Record: A version of this preprint was published at Journal of Molecular Structure on November 1st, 2021. See the published version at https://doi.org/10.1016/j.molstruc.2021.131902.

Abstract

In the present research, a novel mercury (II) metal organic coordination compound, $[Hg(Q)I_2]_n$ (Q = pyridine-4-carbaldehyde thiosemicarbazide) with nano rods shape was prepared applying an ultrasonic manner. The synthesized compound was determined with infrared spectroscopy (IR), scanning electron microscopy (SEM), and X-ray diffraction (XRD). In solid state the coordination polymer takes the appearance of a zig-zag 1D polymer. The coordination number of Hg (II) is four by one sulfur atom of organic ligand and three iodine atoms which two of iodine atoms are coordinated to other repeating units, and one of iodine is unattached. The zig-zag 1D chains interact with neighboring chains via poor interactions, making a 3D supramolecular metal organic polymer.

1. Introduction

A coordination polymer is a metal-organic or an inorganic polymer structure that has metal cation centers connected by organic ligands, and with repetitive coordination entities spreading in 1, 2, or 3 dimensions [1–3]. Coordination polymers are related to several fields like inorganic and organic chemistry, pharmacology, electrochemistry, biochemistry, and materials science, having many useful applications [4–7]. The coordination compounds due to their properties and applications have found a lot of uses in whole life [8]. According to their composition and structure, we can classify it in different ways, such as classification to dimensional which is one of the important ways of Classification [9, 10]. The coordination polymer structure is very important due to its impact on the functionality of coordination polymers. Its structure is based on the reaction conditions, the organic ligand's structure, and the type of metal [11].

Metals by various oxidation number, some inorganic counter and ions neutral organic ligands play vital role in the structure's stability and ultimate geometric topology. The network stability is affected by a mixture of robust interactions such as metal-ligand coordination bonds, with noncovalent interactions including supramolecular between units and hydrogen bonding. Coordination compounds are made of building block units, the above mentioned ligands and metals. These units' self-assembly aggregation resulted in creation of these substances. Particularly this is very fascinating to cultivate them in 1D, 2D, and 3D representing various features. The frameworks' topology can be affected by utilization of solvent as guest molecules [12–15].

Amongst different metal ions, mercury (II) has various attractive features making it a superior case as a central ion for producing coordination polymer [16–18]. First, Hg possesses the d^{10} configuration of mercury (II) making the ion able to create a diverse mixture of geometries with adopting various coordination numbers and thus generating various kinds of metal-organic coordination polymers [19]. The labile nature of mercury (II)-based complexes is the second feature and reversibility of the bonds between donor atoms from the ligand and mercury (II) causes the crystals to be in highly ordered networks, for instance, one dimensional, two dimensional, as well as three dimensional polymers, becomes possible [20–22].

Our team concentrated on the synthesis and design of metal organic coordination compounds. Recently, we provided reports on the preparation of various nano metal organic coordination compounds [23–28]. Our next step in this regard is to assess the coordination behavior of mercury (II) with pyridine-4-carbaldehyde thiosemicarbazide ligand. The organic ligand's structural chemistry is particularly fascinating owing to its multifunctional coordination manner (Scheme 1). A modest sonochemical synthesis route is described for this metal organic coordination system's nano-structure.

2. Experimental

2.1 Instruments and materials

All chemical compounds were bought from the Aldrich and Merck chemical companies. The IR spectroscopy were acquired on a Bruker Vector 22 FT-IR spectrometer utilizing KBr disks in the limited area of 400–4000 cm^{-1}. An Electrothermal 9000 apparatus determine the melting points. A multiwave ultrasonic generator (Sonicator_3000; Misonix, Inc., Farmingdale, NY, the United States) was applied. A X'pert diffractometer manufactured with Panalytical was used along with monochromatized Cu k_{α} radiation, to conduct X-ray powder diffraction (XPRD) measurements. Mercury 2.4 was utilized for preparing simulated XPRD powder patterns in terms of single crystal data [29].

The selected samples' crystallite sizes were determined utilizing the Scherrer formula. A scanning electron microscope (Hitachi) was employed to assess the samples' morphology after Au coating. Gathering diffraction data for the single crystal was performed on an Xcalibur™ diffractometer (Oxford Diffraction Ltd.) armed with a Sapphire2 CCD detector utilizing ω-scan rotation methods and Mo K_{α} radiation (monochromator Enhance, Oxford Diffraction Ltd.) at 150 K. CrysAlis program package (Oxford Diffraction Ltd.) was utilized to perform cell parameter refinements, data collection, and data reduction [30].

The Scherrer manner was used to estimate the selected samples' crystallite sizes. An Au-coated scanning electron microscope (Hitachi-4200) was employed to characterize the specimens.

To the data of $[Hg(Q)I_2]n$, multi-scan absorption modification merged into the CrysAlis was used. The structure was solved within direct processes via a full matrix weighted least-squares technique (SHELX-2014) (the weight of $w = 1/[\sigma^2(F_o)^2 + (0.035P)^2]$, $P = (F_o^2 + 2F_c^2)/3$), by SHELXS and refined on all F^2 data anisotropically. Molecular exhibits were made applying diamond and Mercury 2.4. The crystal data and arrangement modification for 1 are presented in Table 1, and Table 2 represents the designated bond lengths and angles.

Preparation of pyridine-4-carbaldehyde thiosemicarbazide ligand (Q)

0.752 g of pyridine-4-carbaldehyde was dissolved in ethanol 98% in a 100 mL flask and was added one drop of acetic acid. Shortly after, was added 0.636 g of thiosemicarbazide little by little. As soon as the

amine is added, the color of the solution changes to yellow, which indicates the creation of a Schiff base ligand. Then, the solution with stirring was refluxed for 12 hours. In the end, the crystals were filtered then rinsed with a small quantity of cold ethanol. Scheme 2 shows the Q ligand.

Preparation of $[Hg(Q)I_2]_n$ (I) complex crystals

0.019 g (0.1 mmol) of Q ligand and 0.046 g (0.1 mmol) of mercury iodide (II) were weighed and gently placed at the bottom of the branched tube. Then the methanol solvent was softly added to the reaction and the orifice of the tube was blocked with parafilm and placed in the oil bath at 60°C temperature. No additional anion is needed in this reaction. After one week, the tiny yellow crystals of the complex formed at the bottom of the lateral tube. The reactions performed for the $[Hg(Q)I_2]_n$ complex is named (I). The ratio of the ligand to the metal in this reaction is 1:1.

Figure 2 is a view of the synthesized crystals of the complex (I) taken by a microscope. Experiments show the reproducibility of the reaction. The obtained complex monocrystals were structured, and their IR spectra were obtained. The main peaks of its IR spectrum are as follows:

FT-IR (KBr): vmax = 811,1000,1299,1357,1568,232,3269,3380 cm-1.

Preparation of Bulk form of complex (I)

0.9 g of Q ligand with 0.227 g of iodide mercury (II) was poured into a small flask and was added about 15 ml of solvent (methanol) to it, and we let it stirred with a magnet for at least 30 minutes to obtain a Sediment. If there is no sediment, the system should be closed as reflux system (for at least 2 hours) to form a Sediment. In the tested system, sediment was formed at the same first time. Then we filtered the sediment and check the IR spectrum. The main peaks of its IR spectrum are as follows:

FT-IR (KBr): vmax = 648,812,1299,1357,1569,2933,3271,3382 cm-1.

Preparation of complex (I) nanostructures

To prepare the polyhedral nanostructures of this compound, a mixture of 0.18 g (0.1 mmol) of Q ligand in 10 ml of methanol solvent and 0.4544 g (0.1 mmol) of mercury iodide metallic salt in 10 ml of water Distilled or methanol was exposed to ultrasonic waves for 30 minutes in an ultrasonic bath. The white sediment was obtained and after purification under rapid conditions by an air pump, it was dried in the laboratory oven.

FT-IR (KBr): v_{max} = 648,813,1299,1358,1571,2941,3273,3383 cm^{-1}.

Table 1

Crystal data and structure refinements of complex.

Chemical formula	$C_7H_8HgI_2N_4S$
M_r	634.62
Crystal system, space group	Monoclinic, $P2_1/c$
Temperature (K)	150(2)
a, *b*, *c* (Å)	11.5117(5), 14.5972(6), 7.8441(3)
b (°)	92.859(2)°
V (Å^3)	1316.47(9)
Z	4
Crystal size (mm3)	0.180×0.170×0.120
Theta range for data collection	1.771, 27.570°
Max. and min. transmission	0.7456, 0.5744
R_{int}	0.0252
$(\sin q/l)_{max}$ (Å^{-1})	0.600
R,*wR*2 [*I* > 2s(*I*)]	0.0230, 0.0516
R, *wR*2 (all data)	0.0265, 0.0525
No. of reflections	3038
No. of parameters	140
No. of restraints	0
Absorption correction	Semi-empirical from equivalents
$D\tilde{n}_{max}$, $D\tilde{n}_{min}$ (e Å^{-3})	1.956, -1.531
Goodness-of-fit on F2	1.199

Table 2

Selected bond lengths [Å] and angles [°] for 1.

S(1)-Hg(1)-I(2) 124.50	Hg(1)-S(1) 2/4847
S(1)-Hg(1)-I(1) 119.67	Hg(1)-I(2) 2/7081
I(2)-Hg(1)-I(1) 103.985	Hg(1)-I(1) 2/8037
S(1)-Hg(1)-I(1)#1 96.73	Hg(1)-I(1)#1 2/9940
I(2)-Hg(1)-I(1)#1 100.861	S(1)-C(1) 1/722
I(1)-Hg(1)-I(1)#1 107.915	N(1)-C(1) 1/308
Hg(1)-I(1)-Hg(1)#2 94.021	N(2)-N(3) 1/370
C(1)-S(1)-Hg(1) 107.20	N(2)-C(1) 1/337
C(1)-N(2)-N(3) 118.2	N(3)-C(2) 1/285
C(6)-N(4)-C(5) 116.6	N(4)-C(5) 1/353
N(1)-C(1)-N(2) 118.5	C(3)-C(4) 1/389

3. Results And Discussion

3.1. Investigation of Q ligand

In many carbazone ligands, enol-ketone tautomerization occurs. By tautomerization, hydrogen can bind to sulfur on a nitrogen atom adjacent to thiocarbonyl ligand, and the ligand becomes negatively charged. As shown in Scheme 3, this tautomerization can also take place in the Q ligand, and as a result, the bonding of the ligand to the enolate form is observed in the formation of the complex.

Some physical characteristics of Q ligand are given in Table 3.

Table 3
Some physical characteristics of Q ligand

compound	Molecular formula	Molar mass	color	Melting point	Yield (%)
Q	$C_7H_8N_4S$	180 g/mol	cream	200	80 %

The obtained ligands were identified using FT-IR spectroscopy. Figure 2 shows the FT-IR spectrum of Q ligand.

The results of FT-IR spectroscopy show that the band related to the amide tensile vibration for the Q ligand in the region of 3425.98 cm^{-1} is observed as a sharp band. The most important band observed in the spectrum of Schiff base Q ligands belongs to the imine functional group and the hydrogen on the nitrogen atom N^3 of the ligands. Observing the band related to imine is proof of the formation of a Schiff

Base product. The band corresponding to the imine $v_{C=N}$ for the Q ligand is seen as a sharp band in the region of 1602.13 cm^{-1}.

Due to the structure of the synthetic ligand and the observation of a hydrogen atom attached to the nitrogen of the thiosemicarbazide, it is expected that this ligand will act as a neutral ligand by retaining this hydrogen or act as an anionic ligand by losing this hydrogen. The related band v_{N-H}.

For the Q ligand is observed as a sharp band in the 3162.34 cm^{-1} region. The peak corresponding to $v_{C=S}$ for the Q ligand is observed in the region of 1703.36 cm^{-1}. Due to the structure of the synthetic ligand, it is expected that this ligand will act as a mono-dentate or di-dentate ligand. Scheme 4 shows the coordination method of the synthetic Schiff base ligand to the metallic ion.

Investigation of complexes (I) and (II)

By reacting pyridine-4-carbaldehyde thiosemicarbazide organic ligand with a mixture of mercury (II) iodide and methanol, the novel mercury (II) metal organic coordination compound $[Hg(Q)I_2]_n$ was organized. The compound's nanostructure was obtained by ultrasonic irradiation within a methanolic solution, then, the single crystalline substance was attained by utilizing the heat gradients to the reagents solution or the branched tube route. Scheme 5 presented an outline of the routes applied for the preparation of $[Hg(Q)I_2]_n$ applying the two different methods.

Figure 3 shows the complex's FT-IR spectra in the crystalline, bulk, and nano shape. Comparison of these spectra shows their similarity and the corresponding main peaks have a good overlap with each other.

In the FT-IR spectrum of these compounds, absorption bands with varying intensities in the region of 1400–1600 cm^{-1} are attributed to the vibrations of the ligand pyridine ring, which is related to the C = C and C = N bonds. Peaks related to imine C = N are seen as sharp bands in the region of 1600 cm^{-1}, which have shifted to lower wavenumbers by the coordination of the ligand to the metal and the formation of a complex with little displacement.

The tensile N-H peaks in the vibrational spectrum of the complex are observed in the area of 3270 cm^{-1} and indicate the presence of the N-H group of the ligand when it is coordinated with the central metal, and indicate the presence of the ligand in the neutral form in the formation of the complex. For all three complexes, the related band of new C = N bond formation is not observed, and this proves that in the formation of all three complexes Q ligand has participated in the form of ketones in the coordination of metallic ion. The S = C group in the complex is observed in the area of about 1700 cm-1 with a slight displacement which indicates that it is coordinated to the metal.

The N-N group is observed in the 1000 cm^{-1} area that this adsorption band is shifted in the spectrum of all three complexes to lower wavenumbers than the spectrum of ligand, which indicates the lack of coordination of the nitrogen atom of azomethine to the metallic ion. The decrease in v_{N-N} in the

absorption spectrum of the complexes is due to the decrease of bond property in the double bond, which confirms the coordination of the ligand through the sulfur of thiosemicarbazide to the metallic ion.

The results of these studies indicate that if ligand tautomerization takes place, the ligand participates in the formation of complexes in the form of enol, and in the spectrum of complexes the absorption band of v_{N-N} is removed, and v_{C-N} and v_{N-N} shifts to higher numbers and a new C = N bond is created in the wavenumber 1510–1560 cm^{-1}. However, the observation of v_{N-N} band in the spectrum of complexes indicates that the ligand is not tautomerized in the solid-state and the presence of the ketonic form of the ligand in coordination with the metallic ion.

The v_{C-H} aromatic bending is observed in the area of 930 cm^{-1}, and v_{C-C} aromatic bending is observed in the area of 1410 cm^{-1}, and v_{C-H} of the complex aromatic tensile in the area of 3170 cm^{-1} with a slight displacement, indicating that it is coordinated to the metal.

As can be seen, there is a good match between the crystal, nanomaterial, and synthesized bulk in all areas.

The experimental (obtained of the sonochemically prepared specimen) and simulated (achieved with the single crystal arrangement of (I)) powder X-ray diffraction (XRD) patterns were compared and it was proved that based on the crystal structure, the sonochemical manner-produced structured compound is the same as the compound obtained with single crystal diffraction (Fig. 4).

Figure 5 demonstrate the nano rods found with scanning electron microscope. The coordination polymer synthesized with the sonochemical has a very interesting structure. It contains cross-rods by thickness 25-30nm. Further investigations are required for the mechanism of this structure's formation, nevertheless, it may be caused by the complex's crystal structure as a 1D chain. Indeed, packing the structure over a molecular level might affect the morphology of the complex's nano structure.

In Fig. 6, determining the structure by X-ray diffraction indicates that the complex (I) in the solid-state is as a stepped one-dimensional coordination polymer. And the ligand has attached as the monodentate to the mercury metal via the sulfur atom. This complex with Z = 4, is crystallized in the monoclinic crystal lattice and belongs to the spatial group $P2_1/c$. The desired density is 3.3202 Mg/m^3 and the crystal size is 0.12×0.17×0.18 mm^3.

a, b, c are equal to 11.51, 14.59, and 7.84 Å, respectively. Alpha and gamma are equal to 90° and beta is equal to 92.85°. The crystallographic data of the complex are given in Table 4.

Table 4
Crystallography data of the coordination polymer

	x	y	Z	U(eq)
Hg(1)	4432(1)	8054(1)	4875(1)	21(1)
I(1)	3261(1)	6620(1)	6434(1)	18(1)
I(2)	3769(1)	9568(1)	6572(1)	19(1)
S(1)	6417(1)	7796(1)	3867(2)	16(1)
N(1)	6262(4)	5986(3)	4439(6)	21(1)
N(2)	7930(4)	6694(3)	5392(6)	12(1)
N(3)	8341(3)	5852(3)	5904(5)	12(1)
N(4)	10814(4)	3320(3)	8526(6)	20(1)
C(1)	6871(4)	6739(3)	4616(6)	13(1)
C(2)	9329(4)	5843(3)	6743(7)	14(1)
C(3)	9830(4)	4970(3)	7329(6)	14(1)
C(4)	9254(4)	4143(4)	7047(8)	20(1)
C(5)	9768(5)	3349(4)	7661(8)	23(1)
C(6)	11357(4)	4117(4)	8780(7)	18(1)
C(7)	10893(4)	4955(4)	8230(7)	18(1)

Atomic coordinates (x 104) and equivalent isotropic displacement parameters (2x 103) for d1922a_a. U(eq) is defined as one third of the trace of the orthogonalized Uij tensor.

In the unit cell view of this complex (Fig. 7), four structural units with repeating units can be seen that the relationship between these structural units is through the Symmetric elements of screwy axes of 2_1, sliding plates, and centers of symmetry. As shown in Fig. 8, the screwy axes 2_1 are parallel to axis b and the two sliding planes are perpendicular to axis b. The centers of symmetry in the center of a unit cell connect these units to each other.

In this structure, a type of mercury with an asymmetric coordination sphere is observed. In this compound, each mercury central metal has attached to a sulfur atom of Q ligands and three iodine atoms which two of iodine atoms are attached to other repeating units, and one of them is free. Therefore, mercury has a coordination number of 4 with the $HgSI_3$ pattern. In Coordination polymers (I), Communication between structural units is through one bond of Hg-I which has located in bridge mode that caused the formation of the polymeric structure.

The longest bond length with a size of 2.99 Å is related to the Hg-I bond which is in the bridge position and the shortest bond length with a size of 88 is related to the N-H bond. The molecule has no center of symmetry and the lengths of the mercury-iodine bonds are not the same. Also, the angles around the central metal atom are not the same in the coordination cortex, the angles for the three iodine atoms with the central metal and the ligand are about 124.5˚, 119.67˚, 96.73˚. The Q Ligand is coordinated to the central metal via sulfur of thiosemicarbazide and acts as a monodentate ligand in the polymer structure. This compound in solid form is a one-dimensional coordination polymer. The polymeric structure of the compound is shown in Fig. 9.

In coordination polymer, in addition to coordination covalent strong bonds which cause the polymer to expand in a one-dimensional step, other weak interactions such as hydrogen interactions and aromatic interactions cause the self-aggregation of one-dimensional chains and transform the structure into a three-dimensional super molecule with intermolecular interactions.

The structure of the composition is a one-dimensional coordination polymer without considering weak interactions. By considering the weak interactions, the presence of four hydrogen bonds for this structure is observed and becomes a three-dimensional structure which in Fig. 10 show the structure of the complex (I) with Considering the hydrogen bonds and short connections along the b and c axes. Table 5 also shows hydrogen bonds.

Table 5

Selected non-covalent contacts in the crystal structure of (I) [Å and ˚].

D-H...A	d(D-H)	d(H...A)	d(D...A)	<(DHA)
N(1)-H(1NA)...I(1)#3	0.88	3.21	3.907	138.1
N(1)-H(1NA)...I(2)#4	0.88	3.15	3.753	127.6
N(1)-H(1NB)...I(2)#1	0.88	2.83	3.648	155.5
N(2)-H(2N)...N(4)#5	0.85	2.03	2.885	179

Figure 11 shows how the ligands coordinate with the central metal and create a zigzag structure for the complex (I).

The decomposition of precursor $[Hg(Q)(I)_2]_n$ in oleic acid functioning as a surfactant under air atmosphere at 180°C yields nano-powder of Hg (II) oxide. The XPRD pattern of as-synthesized HgO nano powder is seen in Fig. 12. All the diffraction peaks are matched well with the orthorhombic phase HgO with respect to their positions as found in JCPDS card No. 72-1141.

Figure 13 displays the SEM image of as-prepared HgO nanoparticles. The obtained HgO has the regular nanoparticle shape with diameters of around 20-100nm according to size distribution graph of product.

The XPS spectrum (Fig. 14) confirms the presence of O and Hg in the sample. The binding energy corresponding to the peaks O1s, 4f7/2 and 4f5/2 obtained by XPS analysis is 531.05, 100.76 and 104.59 eV, respectively [31].

The thermal gravimetric (TG) analysis was applied to evaluate the thermal stability of the $[Hg(Q)(I)_2]_n$ **1**. TG was recorded in the temperature range of 20 and 800ºC. The diagram of **1** display that the compound remains stable up to 105ºC, and then decomposes up to 215 ºC. The first weight loss is related to removal of iodide units. The step 2 and 3 in the range 285 ºC to 580 ºC with sharp weight losses is attributed to organic moiety of **1** with a mass loss of about 46.8%. The remained solid around 800 ºC is probably HgO.

4. Conclusions

A nano-structure mercuty(II) coordination compound, $[Hg(Q)I_2]_n$ was prepared with ultrasound aided procedure and it was compared with its crystalline structure. The structural characterization of new coordination polymer was done with elemental SEM, IR spectroscopy, and single-crystal diffraction. Determination of the compound's crystal structure, composition of a central building block, and the stereochemistry were revealed through $[Hg(Q)I_2]_n$ creating the one dimensional coordination polymer in the solid state. In the 1D network structure, the mercury (II) ion adopts HgSI3 distorted square pyramid geometry. Thermolysis of coordination polymer **1** results in HgO nanoparticles. It was found that using high intensity ultrasound is a facile, versatile, and eco-friendly synthetic instrument for the supramolecular coordination compounds.

Declarations

Acknowledgements

Here, the University of Qom and Sayyed Jamaleddin Asadabadi University is thankfully acknowledged for supporting this study. This work was funded by the grant NRF-2019R1A5A8080290 of the National Research Foundation of Korea.

References

1. E.R. Engel, J.L. Scott, Advances in the green chemistry of coordination polymer materials. green chem. **22**, 3693–3715 (2020). https://doi.org/10.1039/D0GC01074J
2. J.R. Xiang Liu, Hamon, Recent developments in penta-, hexa- and heptadentate Schiff base ligands and their metal complexes. Coord. Chem. Rev. **389**, 94–118 (2019). https://doi.org/10.1016/j.ccr.2019.03.010
3. M.Y. Masoomi, A. Morsali, Applications of metal–organic coordination polymers as precursors for preparation of nano-materials. Coord. Chem. Rev. **256**, 2921–2943 (2012).

http://dx.doi.org/10.1016/j.ccr.2012.05.032

4. X.R. Wang, X.Z. Wang, Y. Li, K. Liu, S.X. Liu, J. Du, Z. Huang, Y. Luo, J.Z. Huo, X.X. Wu, Y.Y. Liu, B. Ding, Sonochemical Synthesis of A Multi-Responsive Regenerable Water-Stable Zinc(II) Fluorescent Probe for Highly Selective, Sensitive and Real-Time Sensing of Benzaldehyde, Ferric ion and PH, Ultrason Sonochem. 44 (2018) 340–349. https://doi.org/10.1016/j.ultsonch.2018.02.048
5. X. Hu, H. Zhu, X. Sang, D. Wang, Design and Synthesis of Zirconium-Containing Coordination Polymer Based on Unsymmetric Indolyl Dicarboxylic Acid and Catalytic Application on Borrowing Hydrogen Reaction, Adv. Synth. Catal. **360**, 4293–4300 (2018). http://dx.doi.org/10.1002/adsc.201800875
6. K.A. McDonald, S. Seth, A.J. Matzger, Coordination Polymers with High Energy Density: An Emerging Class of Explosives. Cryst. Growth Des. **15**, 5963–5972 (2015). https://doi.org/10.1021/acs.cgd.5b01436
7. R. Haldara, T. Kumar, Metal-organic frameworks (MOFs) based on mixed linker systems: Structural diversities towards functional materials, CrystEngComm. 15 (2013) 9276–9295
8. https://doi.org/10.1039/C3CE41438H
9. F. Novio, J. Simmchen, N. Vazquez-Mera, L. Amorin-Ferre, D. Ruiz-Molina, Coordination polymer nanoparticles in medicine. Coord. Chem. Rev. **257**, 2839–2847 (2013). http://dx.doi.org/10.1016/j.ccr.2013.04.022
10. J.W. Cui, Y.H. Li, L.Y. Zhao, G.H. Cui, Photoluminescence, electrochemical behavior and photocatalytic activities of cobalt(II) coordination polymer nanostructures synthesized by sonochemical process. Ultrason Sonochem. **39**, 837–844 (2017). https://doi.org/10.1016/j.ultsonch.2017.06.004
11. J. Li, X.H. Ji, J.T. Li, Two new inorganic anions directed Zn(II)-tetrazole frameworks: Syntheses, structures and photoluminescent properties. J. Mol. Struct. **1147**, 22–25 (2017). http://dx.doi.org/10.1016/j.molstruc.2017.06.089
12. H.Y. Lin, J. Luan, X.L. Wang, J.W. Zhang, G.C. Liu, A.X. Tian, Construction and properties of cobalt(II)/copper(II) coordination polymers based on N-donor ligands and polycarboxylates mixed ligands. RSC Adv. **4**, 62430–62445 (2014). https://doi.org/10.1039/C4RA12367K
13. W. Lu, Z. Wei, Z.Y. Gu, T.F. Liu, J. Park, J. Park, J. Tian, M. Zhang, Q. Zhang, T. Gentle, M. Boscha, H.C. Zhou, Tuning the structure and function of metal–organic frameworks via linker design. Chem. Soc. Rev. **43**, 5561 (2014). https://doi.org/10.1039/c4cs00003j
14. S. Yuan, J.S. Qin, L.F. Zou, Y.P. Chen, X. Wang, Q. Zhang, H.C. Zhou, Thermodynamically Guided Synthesis of Mixed-Linker Zr-MOFs with Enhanced Tunability
15. J. Am, Chem. Soc. **138**, 6636–6642 (2016). https://doi.org/10.1021/jacs.6b03263
16. A. Tabacaru, C. Pettinari, S. Galli, Coordination polymers and metal-organic frameworks built up with poly(tetrazolate) ligands, Coord. Chem. Rev. **372**, 1–30 (2018). https://doi.org/10.1016/j.ccr.2018.05.024
17. Y. Xu, Q. Li, H. Xue, H. Pang, Metal-organic frameworks for direct electrochemical applications. Coord. Chem. Rev. **376**, 292–318 (2018). https://doi.org/10.1016/j.ccr.2018.08.010

18. L.O. Amaral, V.S. Lima, S.M. Soares, J. Bornhorst, S.S. Lemos, C.C. Gatto, R.A. Burrow, P. Gubert, Synthesis, structural characterization and evaluation of the chelating potential in *C. elegans* involving complexes of mercury (II) with Schiffbases derived from amino acids. J. Organomet. Chem. **926**, 121500 (2020). https://doi.org/10.1016/j.jorganchem.2020.121500
19. D.S. Liu, Y. Sui, G.M. Ye, H. Wang, J.Q. Liu, W.T. Chen, Synthesis, structures and properties of three mercury coordination polymers based on 5-methyltetrazolate ligand. J. Solid State Chem. **263**, 182–189 (2018). https://doi.org/10.1016/j.jssc.2018.04.016
20. T. Mocanu, L. Kiss, A. Sava, S. Shova, C. Silvestru, M. Andruh, Coordination polymers and supramolecular solid-state architectures constructed from an organometallic tecton, bis(4-pyridyl)mercury, Polyhedron. 166 (2019) 7–16. https://doi.org/10.1016/j.poly.2019.03.020
21. A. Morsalia, M.Y. Masoomi, Structures and properties of mercury(II) coordination polymers. Coord. Chem. Rev. **253**, 1882–1905 (2009). https://doi.org/10.1016/j.ccr.2009.02.018
22. I. Cabac, D. Davarcı, Y. Zorlu, Ligand effects on the dimensionality of cyclophosphazene-based mercury(II) coordination polymers: Structures, UV–Visible absorption and thermal properties. Polyhedron. **192**, 114823 (2020). https://doi.org/10.1016/j.poly.2020.114823
23. D.M. Chen, X.F. Wu, Y.J. Liu, C. Huang, B.X. Zhu, Synthesis, crystal structures and vapor adsorption properties of Hg(II) and Cd(II) coordination polymers derived from two hydrazone Schiff base ligands. Inorganica Chim. Acta. **494**, 181–186 (2019). https://doi.org/10.1016/j.ica.2019.05.026
24. A. De, A. Sahu, S. Paul, M. Joshi, A.R. Choudhury, B. Biswas, Structural and luminescent properties of a new 1D Cadmium(II) coordination polymer: A combined effort with experiment & theory. J. Mol. Struct. **1167**, 187–193 (2018). https://doi.org/10.1016/j.molstruc.2018.04.081
25. B. Mirtamizdoust, Y. Hanifehpour, E. Behzadfar, M. Sadeghi-Roodsari, J.H. Jung, S.W. Joo, A novel nano-structured three-dimensional supramolecular metal-organic framework for cadmium (II): A new precursor for producing nano cadmium oxide. J. Mol. Struct. **1201**, 127191 (2020). https://doi.org/10.1016/j.molstruc.2019.127191
26. Y. Abbasi Tyula, A. Zabardasti, H. Goudarziafshar, B. Mirtamizdoust, A new hemidirected lead(II) complex extended in holodirected one-dimensional polymer by secondary Pb–O interactions: A precursor for preparation of PbO nanoparticles, and DFT study. J. Mol. Struct. **1149**, 142–148 (2017). https://doi.org/10.1016/j.molstruc.2017.07.090
27. Y. Hanifehpour, B. Mirtamizdoust, M. Hatami, B. Khomami, S.W. Joo, Synthesis and structural characterization of new bismuth (III) nano coordination polymer: A precursor to produce pure phase nano-sized bismuth (III) oxide. J. Mol. Struct. **1091**, 43–48 (2015). http://dx.doi.org/10.1016/j.molstruc.2015.02.074
28. Y. Hanifehpour, A. Morsali, B. Mirtamizdoust, S.W. Joo, Sonochemical synthesis of tri-nuclear lead(II)-azido nano rods coordination polymer with 3,4,7,8-tetramethyl-1,10-phenanthroline(tmph): Crystal structure determination and preparation of nano lead(II)Oxide. J. Mol. Struct. **1079**, 67–73 (2015). http://dx.doi.org/10.1016/j.molstruc.2014.09.016

29. Y. Hanifehpour, J. Dadashi, B. Mirtamizdoust, Ultrasound-Assisted Synthesis and Crystal Structure of Novel 2D Cd (II) Metal–Organic Coordination Polymer with Nitrite End Stop Ligand as a Precursor for Preparation of CdO Nanoparticles. Crystals. **11**, 197 (2021). https://doi.org/10.3390/cryst11020197
30. F. Mojtabazade, B. Mirtamizdoust, A. Morsali, P. Talemi, Sonochemical synthesis and structural determination of novel the nano-card house Cu(II) metal-organic coordination system, Ultrason Sonochem. 35 (2017) 226–232. http://dx.doi.org/10.1016 /j.ultsonch.2016.09.022
31. Mercury 2.4, Copyright Cambridge Crystallographic Data Centre, 12 Union
32. Road, Cambridge, CB2 1EZ, UK, 2001–2010
33. Oxford Diffraction. CrysAlis RED and CrysAlis CCD software (Ver. 1.171.32.5)
34. Oxford Diffraction Ltd.: Abingdon, Oxfordshire, UK, 2003
35. P. Glans, T. Learmonth, K.E. Smith, **Experimental and theoretical study of the electronic structure of HgO and Tl_2O_3**. Phys. Rev. **71(**, 235109 (2005). **PhysRev B. 71.235109**, **)**

Figures

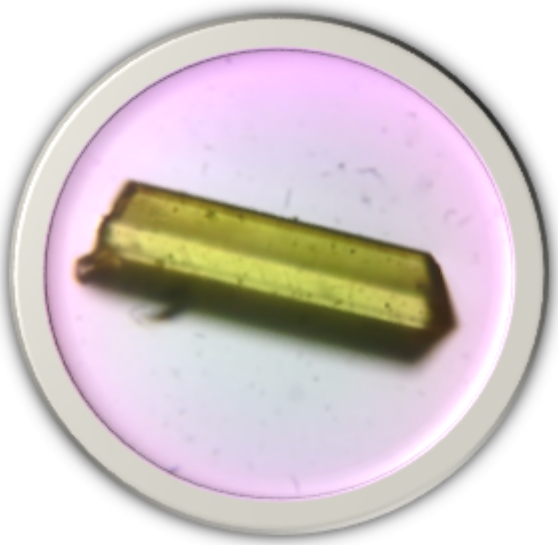

Figure 1

View of the complex crystal (I)

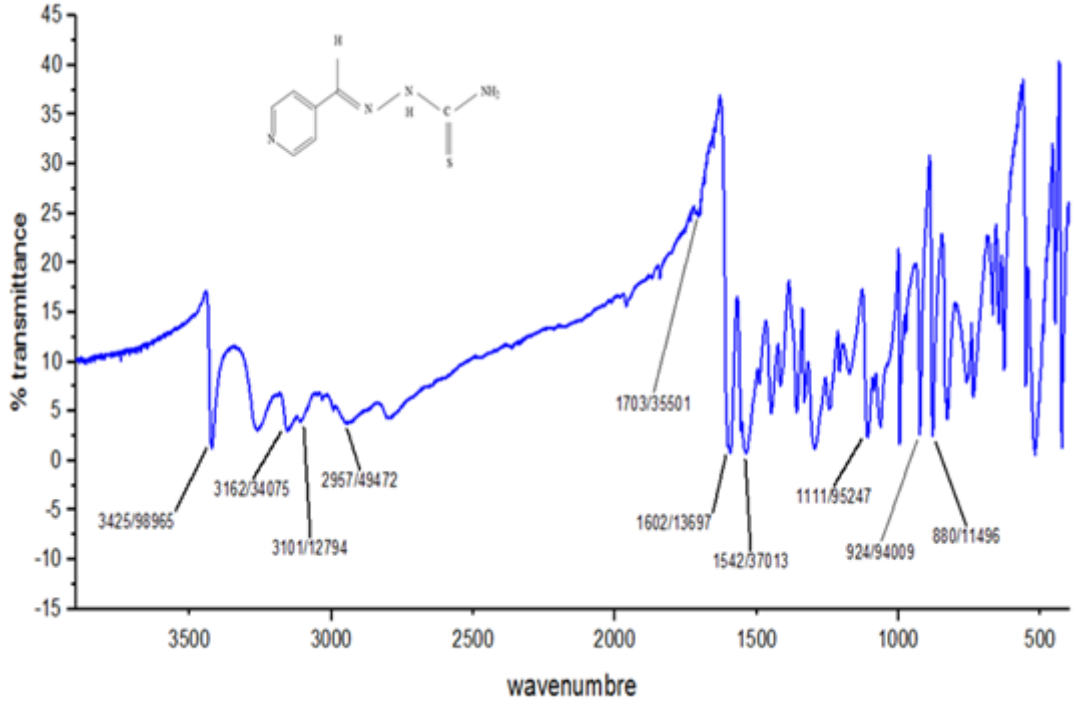

Figure 2

The FT-IR spectrum of Q ligand.

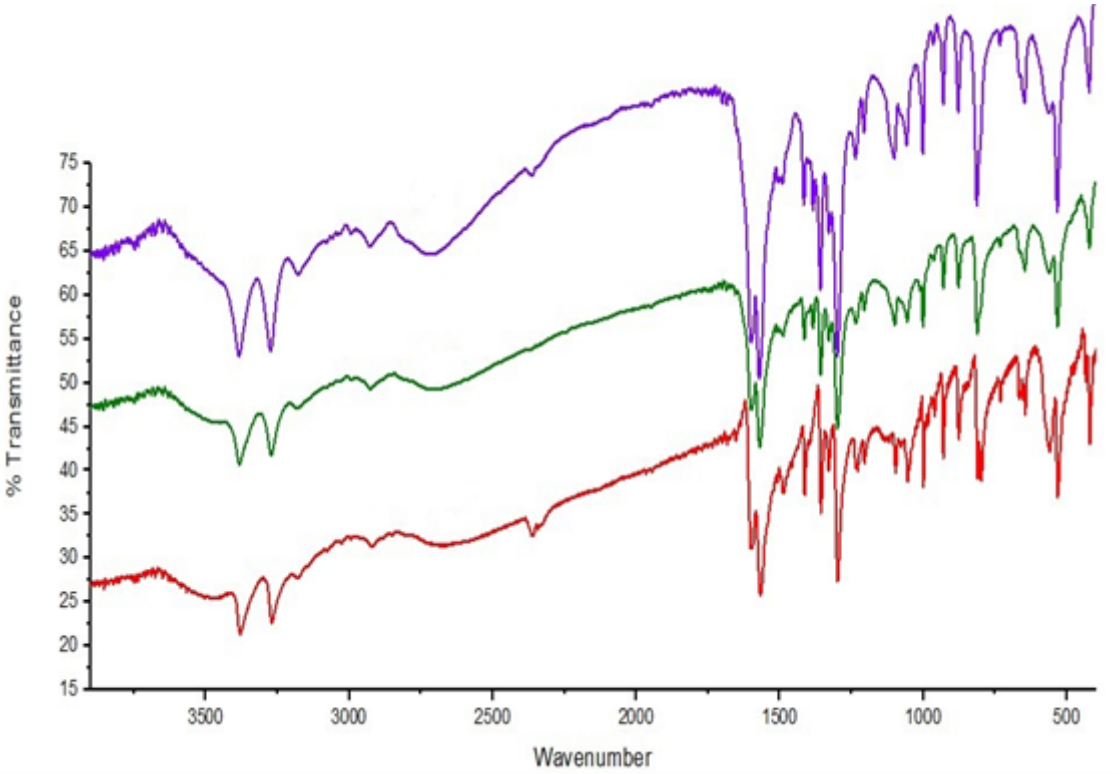

Figure 3

The FT-IR spectra of the [Hg(Q)I2]n (I) complex in the crystalline (Red), bulk Green), and nano shape (Purple).

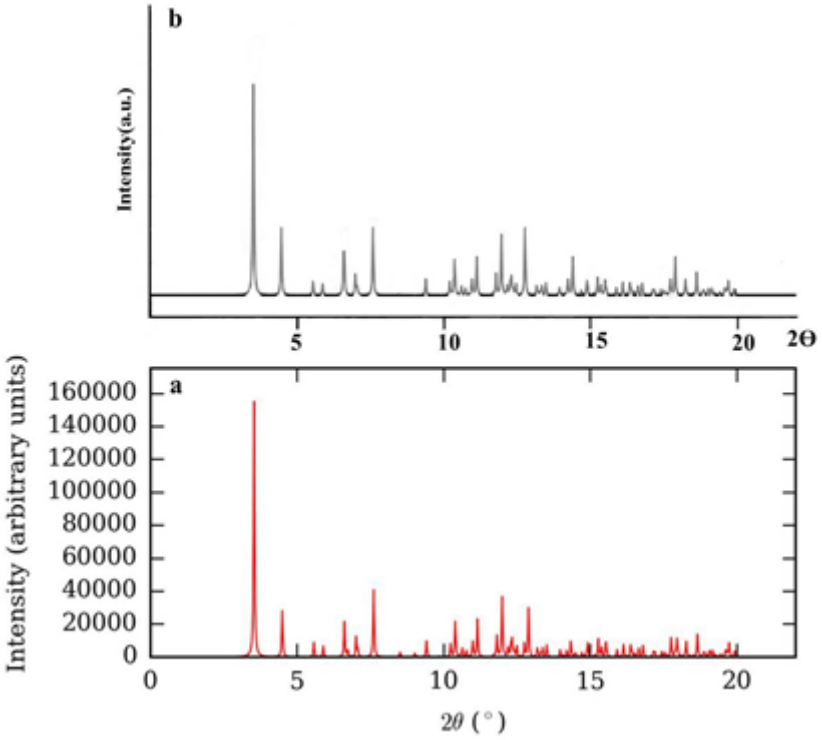

Figure 4

XRD patterns of (a) computed from single crystal X-ray data of compound (I); (b) nano structure of compound (I).

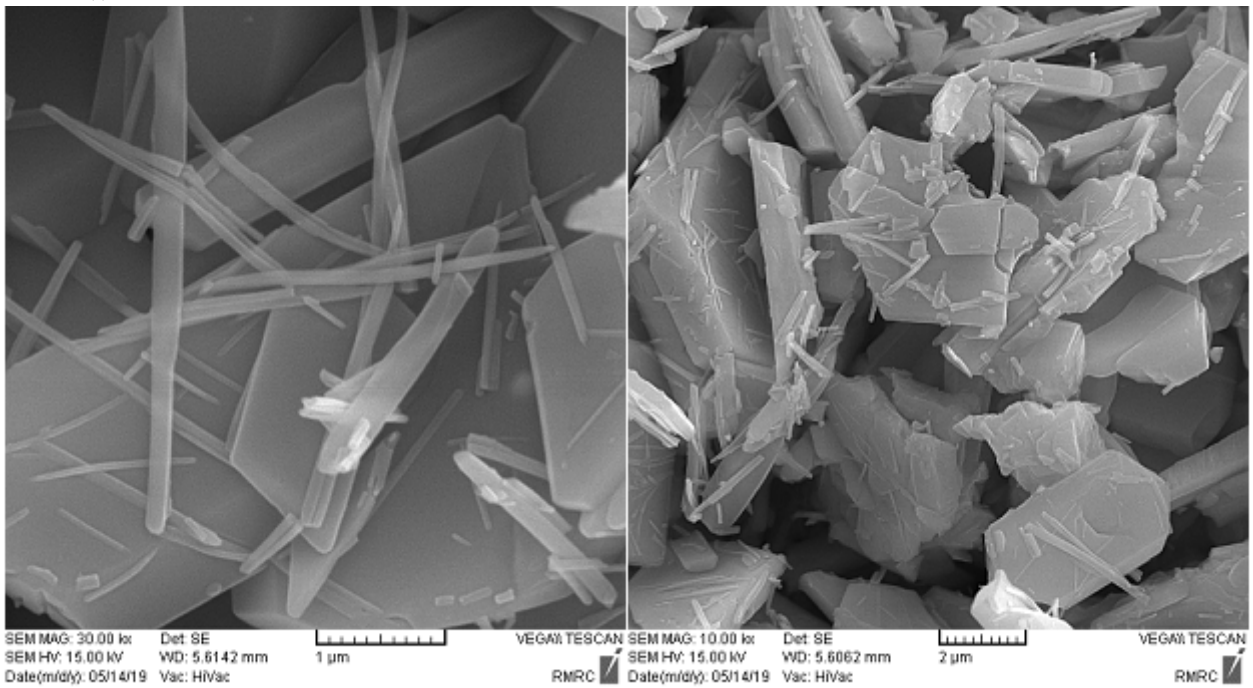

Figure 5

SEM photographs of [Hg(Q)I2]n (I) nano rods.

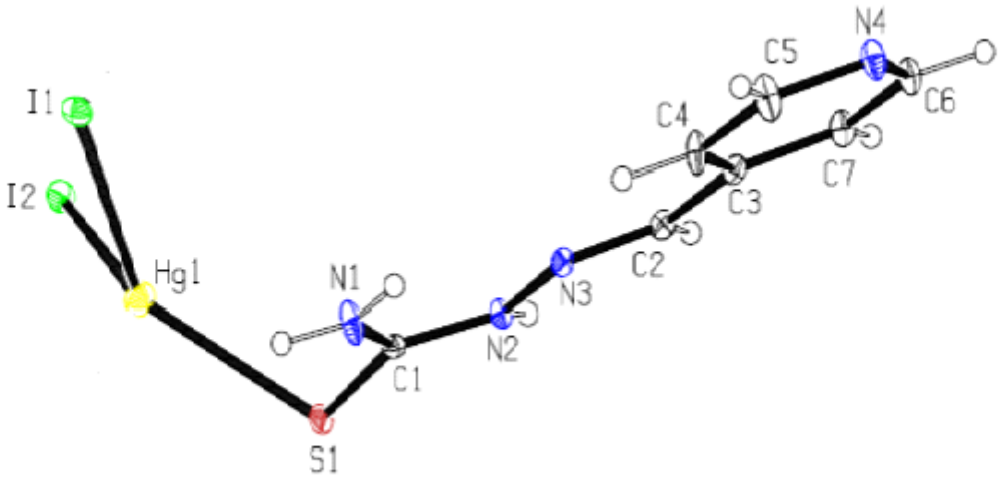

Figure 6

The crystal structure of [Hg(Q)(I)2]n complex(I).

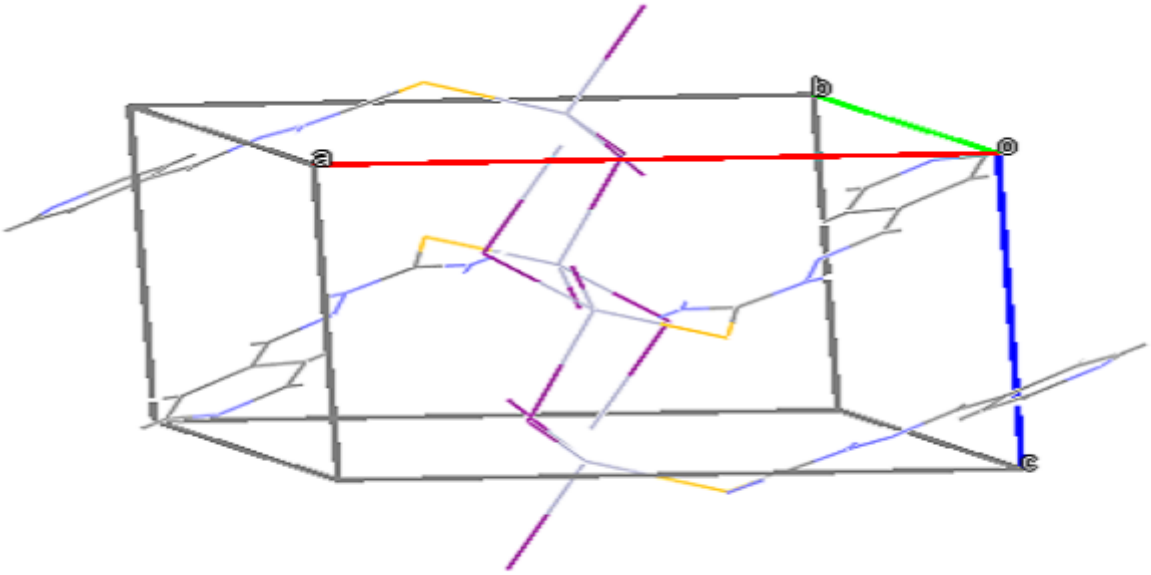

Figure 7

The [Hg(Q)(I)2]n Complex(I) unit cell structure.

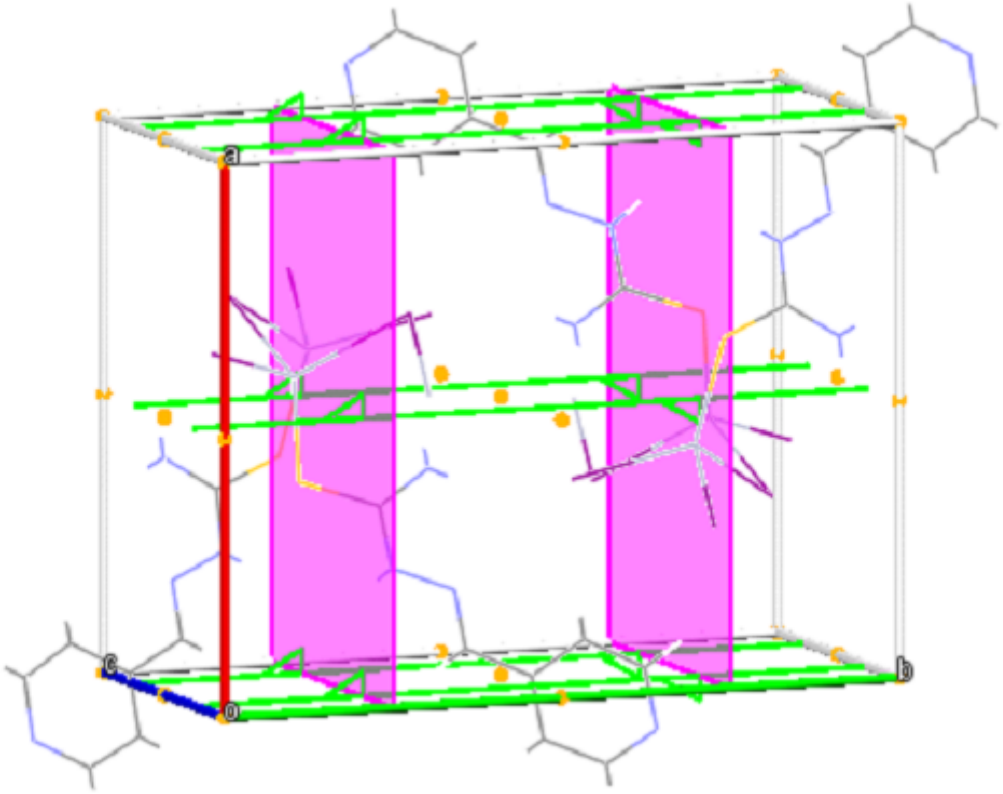

Figure 8

Representation of symmetric elements of complex (I) crystal along the axis C.

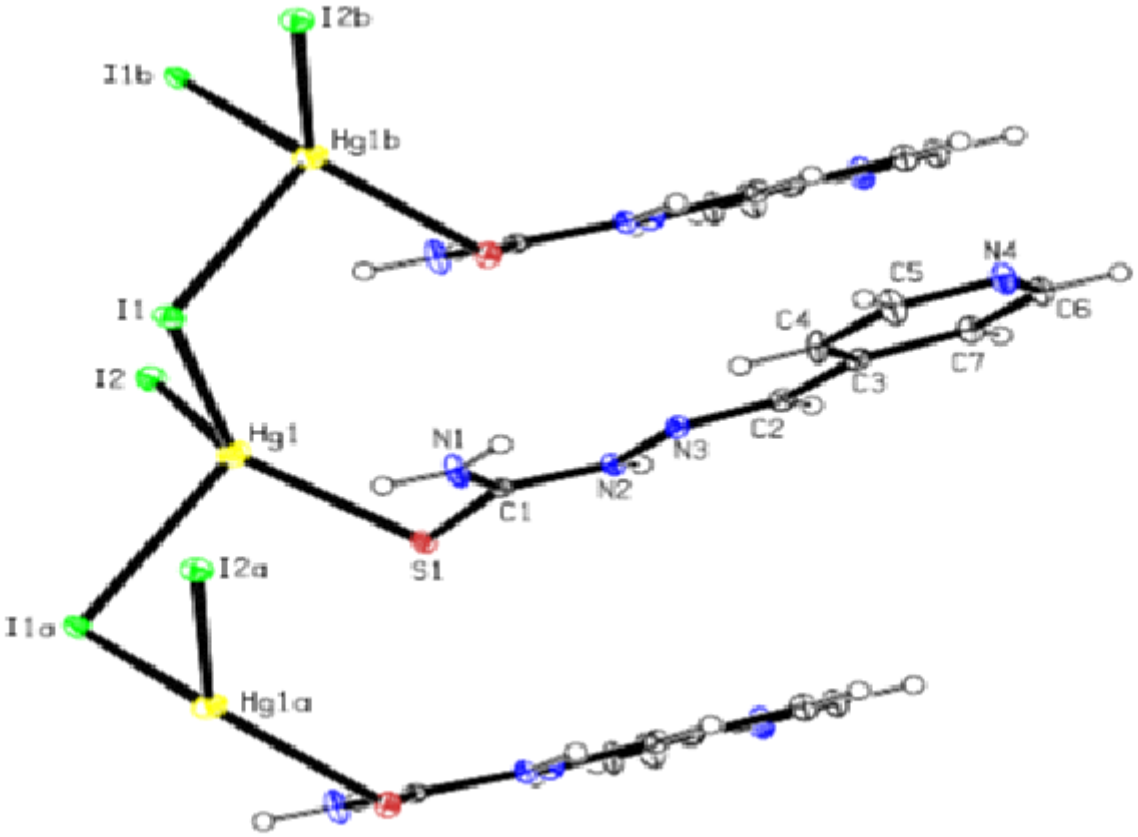

Figure 9

Coordination (I) polymer structure.

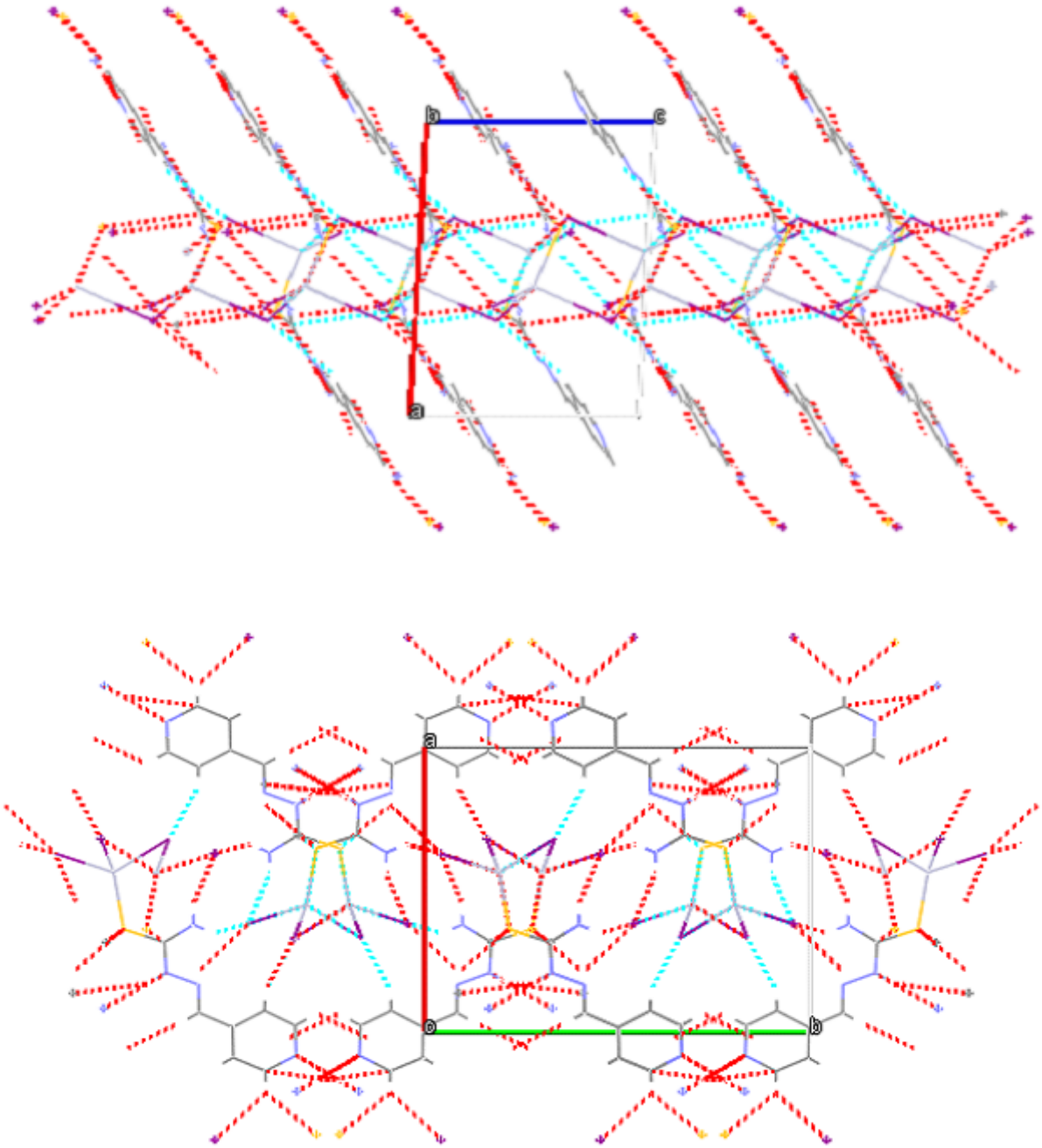

Figure 10

Complex (I) structure considering hydrogen bonds and short connections along axis b (top) and axis c (bottom).

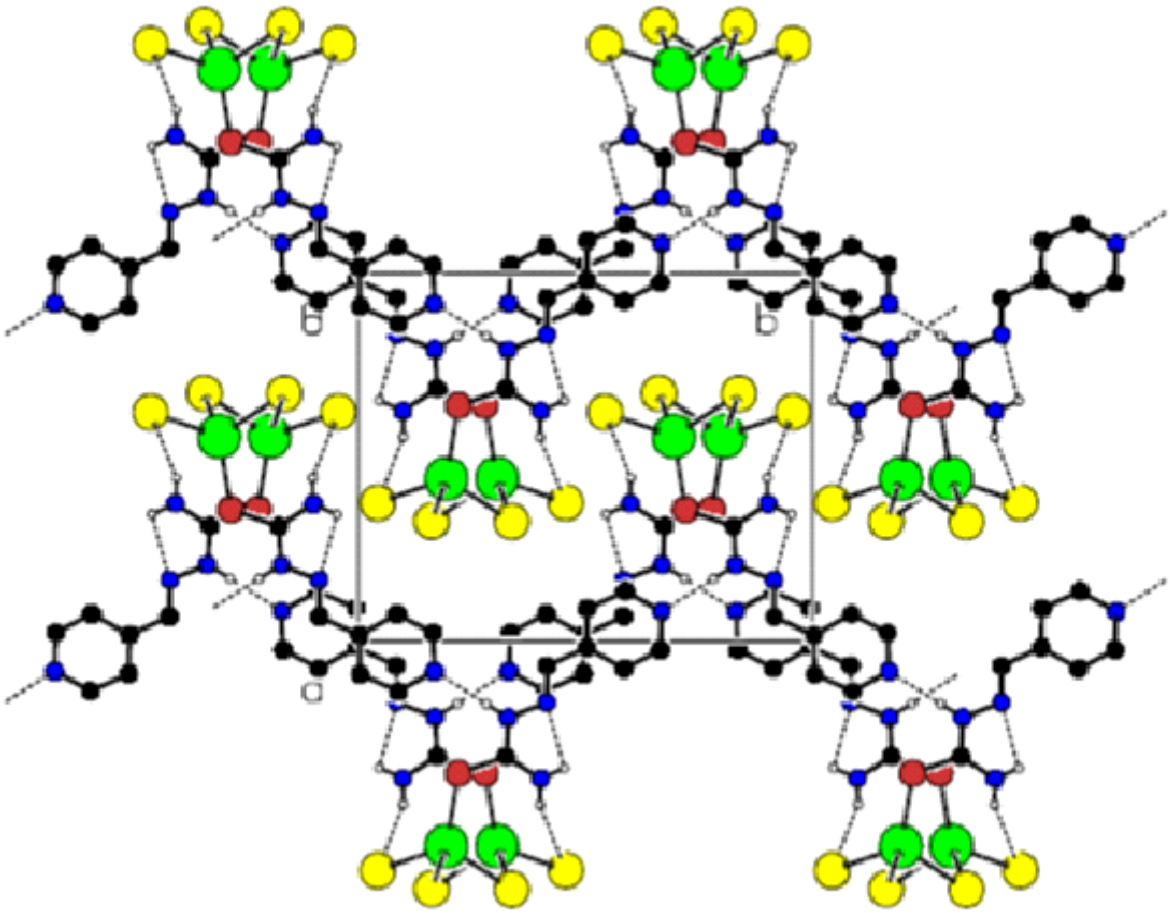

Figure 11

Stacked structure of coordination polymer (I).

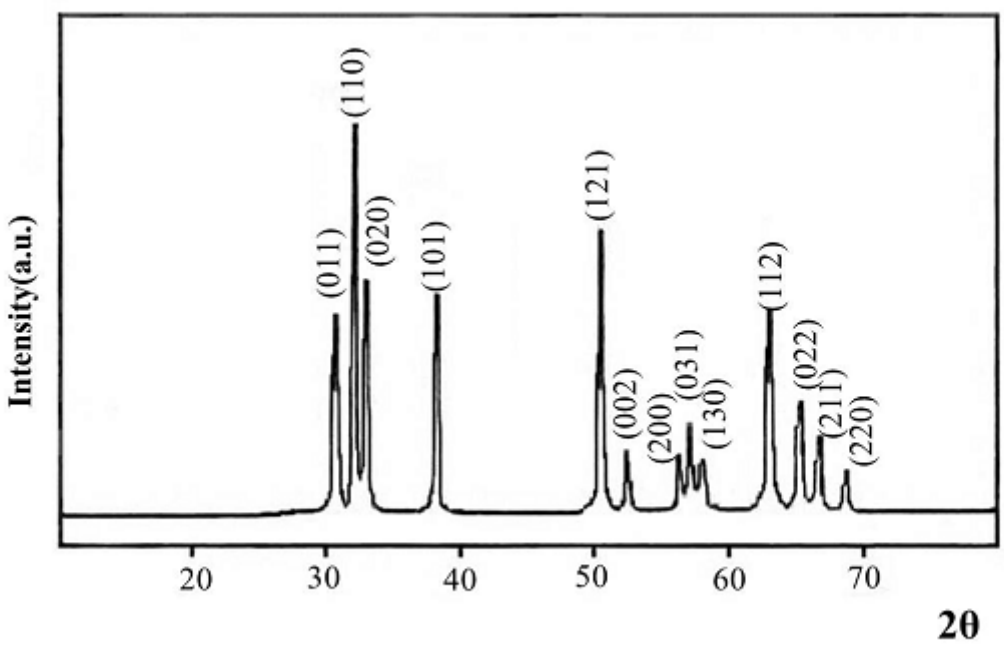

Figure 12

XRD pattern of Mercury oxide prepared by decomposition of (1).

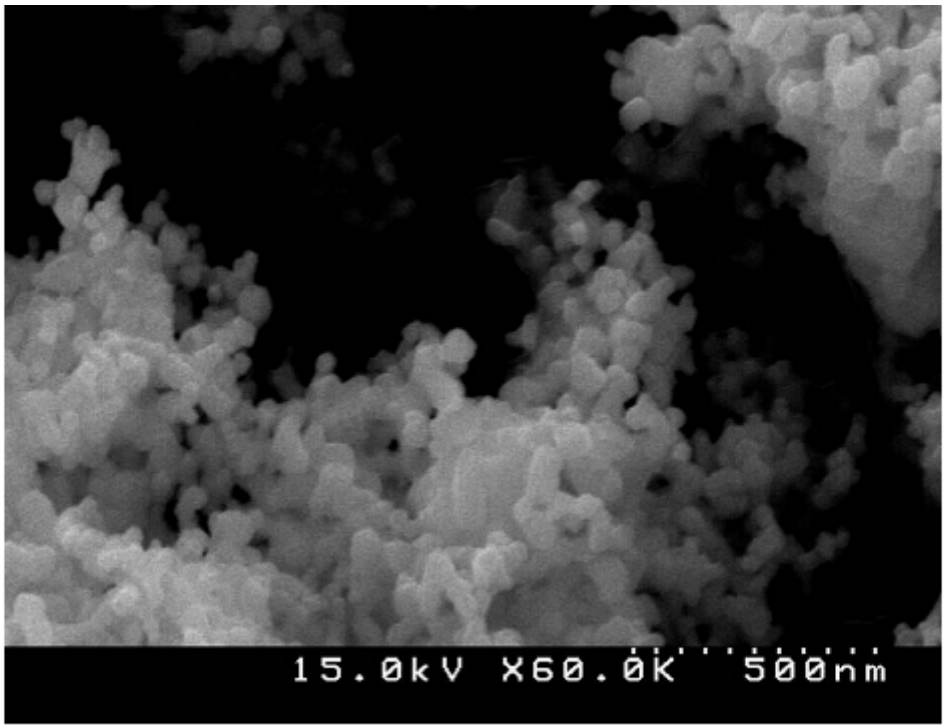

Figure 13

SEM photograph of nano mercury oxide (obtained by thermolyses of precursor 1).

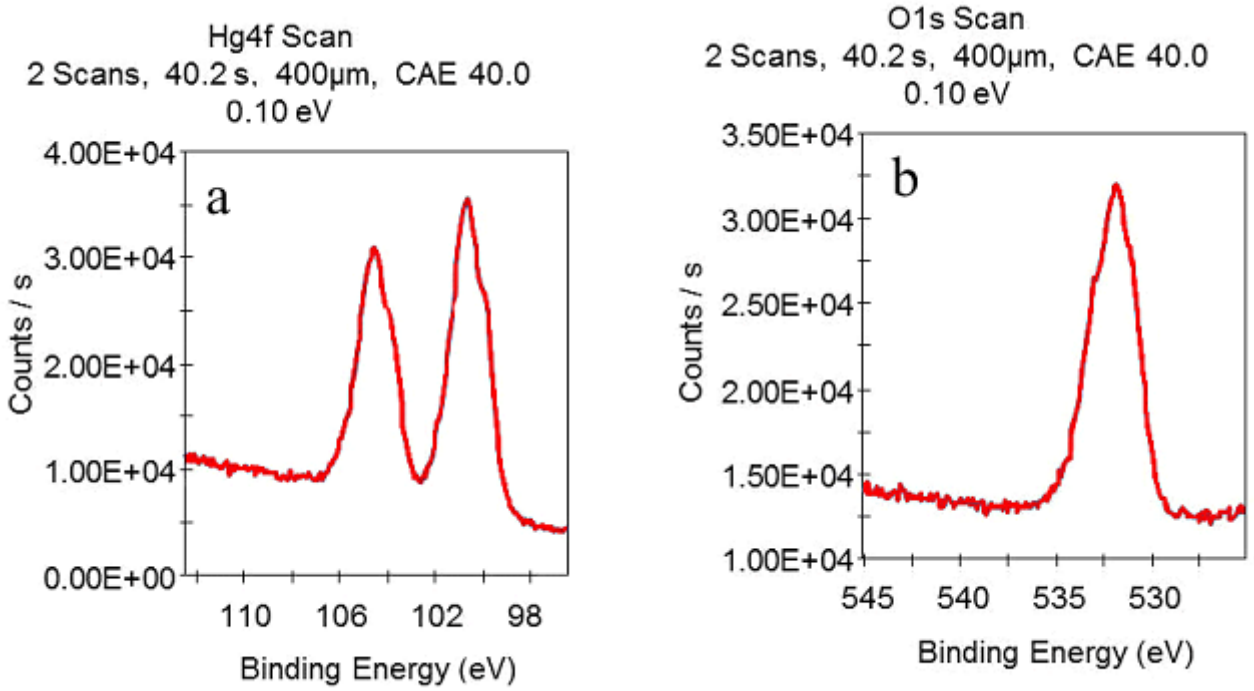

Figure 14

HgO XPS spectra obtained by thermolysis of 1.

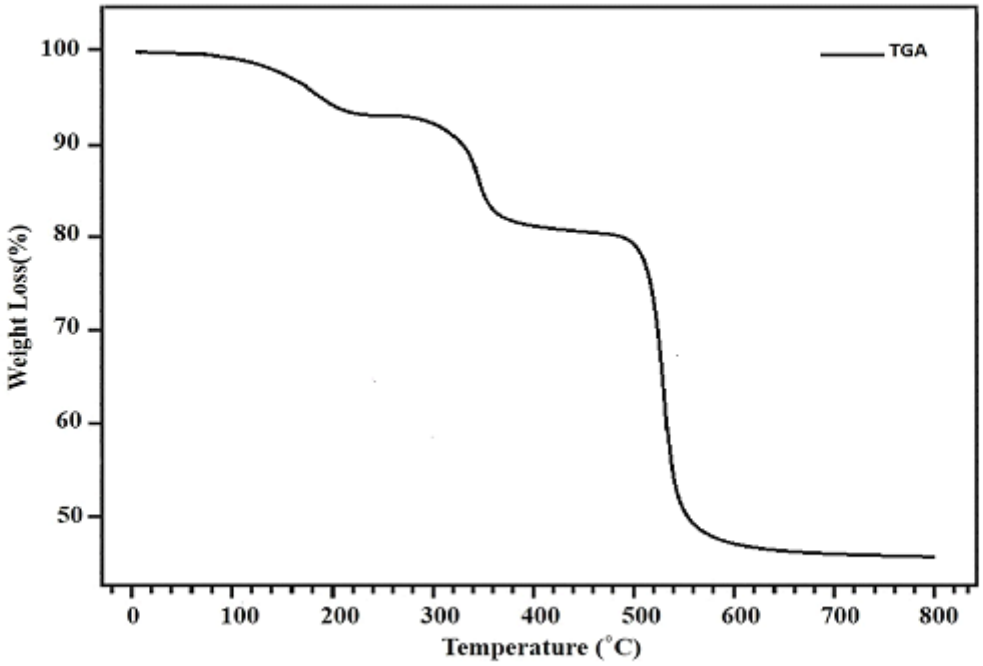

Figure 15

TGA thermogram of [Hg(Q)(I)2]n.

Supplementary Files

This is a list of supplementary files associated with this preprint. Click to download.

- Scheme01.png
- Scheme02.png